

Selection of a whole-cell biocatalyst for methyl parathion biodegradation

Jijian Yang · Ruihua Liu · Hong Jiang · Yao Yang ·
Chuanling Qiao

Received: 18 October 2011 / Revised: 20 November 2011 / Accepted: 23 November 2011 / Published online: 30 December 2011
© Springer-Verlag 2011

Abstract Whole-cell biocatalyst has the potential to become a cost-effective alternative to conventional enzyme methods for solving ecological and energy issues. However, cytosolic-expressing biocatalyst systems are critically disadvantaged due to the low permeability of the cell membrane. To overcome substrate transport barrier, periplasmic secretion and surface display biocatalysts were developed by expressing signal peptides or anchor proteins in *Escherichia coli*. In this work, six carriers were compared in regard to whole-cell activity of methyl parathion hydrolase (MPH). Our results indicate that the surface display systems yielded one to three times whole-cell activity than the periplasmic secretion systems. Although periplasmic secretion systems showed generally more stable than surface display systems, surface display appeared more suitable for whole-cell biocatalyst. It should note that the applicability of the DsbA/PhoA/AIDA-I leader to MPH expression is shown here for the first time. In addition, the result provided a useful reference for other whole-cell biocatalyst selection.

Keywords Methyl parathion hydrolase · Periplasmic secretion · Surface display · Biocatalyst · Biodegradation

Introduction

In recent years, biocatalyst has been becoming a cost-effective technology for solving ecological and energy issues (Chu et al. 2009). Unfortunately, purified biological enzymes tend to be high in cost due to purification procedures, making the process uneconomical (Noureddini et al. 2005). Even with the ability to reuse the enzymes for several reaction cycles by immobilizing the enzyme in or on a physical structure, the cost continues to be high. An alternative to purified enzyme is to use the whole cells that produce the enzyme. Whole cells offer the important advantage of a simple, hence low-cost catalyst preparation.

The microbial degradation of pesticides residues has become the focus of many studies because it is economical and effective. Thereamong, organophosphorus (OPs)-degrading (*opd*) and methyl parathion-degrading (*mpd*) genes have been intensively researched (Fu et al. 2004; Rani and Lalithakumari 1994; Yang et al. 2006; Zhang et al. 2006). In the case of cytosolic-expressing biocatalyst, the outer membrane acting as a substrate diffusion barrier prevents OPs from interacting with organophosphorus hydrolase (OPH) residing within the cell. Therefore, attempts had been made to enhance OPH biodegradation efficiency by displaying the OPH onto the cell surface (Richins et al. 1997; Yang et al. 2008) or by secreting the OPH into the periplasmic space (Kang et al. 2006; Yang et al. 2009). Richins reported firstly that OPH could be displayed and anchored onto the surface of *Escherichia coli* using an Lpp–OmpA fusion system (Richard et al. 1997). In their work, more than 80% of the OPH activity was located on the cell

J. Yang
Taishan University,
Shandong 271021, China

J. Yang · H. Jiang · Y. Yang · C. Qiao (✉)
State Key Laboratory of Integrated Management of Pest Insects
and Rodents, Institute of Zoology, Chinese Academy of Sciences,
Da Tun Lu,
Beijing 100101, People's Republic of China
e-mail: qiaocl@ioz.ac.cn

R. Liu
College of Pharmacy and Tianjin Key Laboratory of Molecular
Drug Research, Nankai University,
Tianjin 300071, China

surface as determined by protease accessibility experiments. Whole cells expressing OPH on the cell surface degraded parathion and paraoxon very effectively without any diffusional limitation, resulting in sevenfold higher rates of parathion degradation when comparing with intracellular OPH. In another recent study with methyl parathion hydrolase (MPH), the recombinant strain translocating MPH to the periplasm by employing the twin-arginine translocation (Tat) pathway showed sixfold higher whole-cell activity than the control strain expressing cytosolic OP hydrolases (Yang et al. 2010). Other studies documenting the whole-cell biocatalysts activity have been reported (Bae et al. 2003; Katahira et al. 2006; Lee et al. 2006; Qin et al. 2006; Shigechi et al. 2004).

However, so far we cannot tell which whole-cell catalysts system is more applicable for organophosphorus detoxification. In all published paper, there was no systematic comparison between periplasmic secretion and surface displaying under similar experimental condition. In the present work, *E. coli* cell, expressing MPH in different compartments (cytoplasm, periplasm, and surface), was used as whole-cell catalyst for detoxifying OPs. We analyzed the influence of various carrier peptides on whole-cell activity. Secretion (Sec) pathway, signal recognition particle (SRP) pathway, and Tat pathway were compared. Various surface-anchoring motifs, such as the lipoprotein-outer membrane protein A chimera (Lpp-OmpA), ice nucleation protein (InaV), and autotransporter AIDA-1, were also compared in this work. We aimed to achieve functional application of MPH and eventually explore the best way to exploit the whole-cell biocatalyst.

Materials and methods

Plasmid constructions

Standard cloning procedures were performed according to Sambrook and Russell (2003). To generate vectors expressing periplasmic MPH, *mpd* gene was polymerase chain reaction (PCR) amplified from plasmid pUM18 using primers P1 and P2 (Table 1). The product was digested with *Bam*HI and *Hind*III and cloned into plasmid pUC18 to generate vector pUMb. The *DsbA* leader peptides was PCR amplified (P3 and P4) from the *E. coli* K-12 chromosomal DNA and subcloned into pUMb with *Eco*RI-*Bam*HI to generate pUDM18. To construct periplasmic expression vector coding for PhoA-MPH fusion, the PhoA leader peptides was amplified from the genomic DNA of *E. coli* K-12 using primers P5 and P6 based on the GenBank sequence (GenBank J01659.2), digested with *Eco*RI-*Bam*HI, and ligated into similarly digested pUMb to generate pUPM18. pUTM18 was used as the periplasmic-secretion vector coding for TorA-MPH fusion.

For surface display of MPH, the *inpnc-mpd* fusion gene was PCR amplified from pINCM using primers P7 and P8, digested with *Eco*RI/*Hind*III, and ligated into similarly digested pUC18 to generate pINCM18. The *lpp-ompA* fusion gene was digested with *Eco*RI and *Bam*HI from plasmid pLO, then ligated into similarly digested pUMb to generate pULOM18. The signal peptide coding region of AIDA-I (49 aa) was amplified by PCR from plasmid pDT1 with primers P9 and P10. The fragment was digested with *Eco*RI and *Kpn*I and ligated into a similarly digested pUC18, resulting in pUP. The *mpd* gene was amplified by PCR using primers P11 and P12 from plasmid pUM18. An encoding fragment without termination codon was digested by *Kpn*I and *Bam*HI and inserted into a correspondingly digested pUP to generate pUPM. Finally, the linker region and the β -barrel coding region of AIDA was amplified by PCR using primers P13 and P14 from plasmid pDT1. The 1.5-kb fragment was digested by *Bam*HI-*Hind*III and ligated into an equally digested pUPM to generate pUADM18.

pUM18 was used as a control plasmid for expressing the MPH fusion protein in the cytoplasm. All plasmid constructs were verified by DNA sequence analysis. Transformation of plasmid into *E. coli* was carried out using the CaCl₂ method (Sambrook and Russell 2003).

Strain and growth condition

All plasmids and primers used in this study are listed in Table 1. *E. coli* DH5 α was used for constructing recombinant plasmids. JM109, XL1-Blue, BL21(DE3), and UT5600 were used as a host for recombinant protein expression. All *E. coli* cells carrying plasmids were grown in Luria-Bertani (LB) medium supplemented with ampicillin (100 μ g ml⁻¹) at 250 rpm and 37 °C. When the culture reached an optical density at 600 nm (OD₆₀₀) of 0.5, 0.1 mM isopropyl- β -D-thiogalactopyranoside (IPTG) was added to the culture broth for induction of recombinant protein expression. After IPTG induction, cells were incubated at 250 rpm and 30 °C for 24 h.

Cell fractionation

To demonstrate periplasmic secretion of MPH, cells were fractionated to obtain shocked cell and periplasmic fractions by the cold osmotic shock procedure (DeLisa et al. 2003; Thomas et al. 2001). After disruption of the shocked cells by sonication and a brief clarifying spin, the clarified lysate was ultracentrifuged at 50,000 rpm for 1 h at 4 °C, and the supernatant was retained as the cytoplasmic fraction. To verify the surface localization of MPH, cells were fractionated into a soluble fraction and an outer membrane fraction as described previously (Li et al. 2004).

Table 1 Plasmids and primers used in this work

Plasmid and primers	Description	Source or reference
Plasmids		
pUC18	pUC origin of replication, <i>lac</i> promoter, Apr	This lab
pDT1	5.5-kb Amp ^r encodes signal peptide and the AIDA translocator	Li et al. 2008
pINCM	Source of gene coding INPNC–MPH fusion	Yang et al. 2008
pLO	Source of gene coding <i>lpp</i> – <i>ompA</i> fusion	Yang et al. 2008
pUM18	pUC18 derivative, control plasmid for expressing a cytosolic MPH	Yang et al. 2010
pUTM18	pUC18 derivative, periplasmic secretion vector coding for TorA–MPH fusion	Yang et al. 2010
pUDM18	pUC18 derivative, periplasmic secretion vector coding for DsbA–MPH fusion	This study
pUPM18	pUC18 derivative, periplasmic secretion vector coding for PhoA–MPH fusion	This study
pUADM18	pUC18 derivative, surface display vector coding for AIDA–MPH fusion	This study
pULOM18	pUC18 derivative, surface display vector coding for <i>lpp</i> – <i>ompA</i> –MPH fusion	This study
pINCM18	pUC18 derivative, surface display vector coding for INPNC–MPH fusion	This study
Primers		
	5'→3'	
P1	<u>GGATCCC</u> CGCCGACCAGGTGCGC	This study
P2	<u>AAGCTTC</u> ACTTGGGGTTGACGAC	This study
P3	<u>ACGAATTC</u> GATGAAAAAGATTGGC	This study
P4	<u>GGATCC</u> CTGCGCCGCC	This study
P5	<u>GAATTC</u> CGTGAAACAAAGCACTATTG	This study
P6	<u>GGATCC</u> TGTCCGGGCTTTTGTC	This study
P7	<u>GAATTC</u> CATGAATATCGACAAAGCGTTG	This study
P8	<u>AAGCTTC</u> ACTTGGGGTTGACGACCG	This study
P9	<u>GCGAATTC</u> AGGAAACAATGAATAAGGCCTACAGTATC	This study
P10	<u>GCGGTACCC</u> ATTGCAAATGCATTTCCGATTG	This study
P11	<u>GGTACCATG</u> CCCGCACCAGGTGCGC	This study
P12	<u>GGATCC</u> CTTGGGGTTGACGACCG	This study
P13	<u>GGGGATCCA</u> ATAACAATGGAAGCAT	This study
P14	<u>CCAAGCTTC</u> AGAAGCTGTATTTTATC	This study

The restriction sites are underlined

SDS-PAGE and western blot

Subcellular fractionated samples were analyzed by sodium dodecyl sulfate–polyacrylamide gel electrophoresis (SDS-PAGE) with 12% (*w/v*) acrylamide (Sambrook and Russell 2003). For Western blot analysis, the gel was transferred onto nitrocellulose membranes (Millipore) with a tank transfer system (Bio-Rad). After nonspecific binding sites were blocked with 3% bovine serum albumin in TBST buffer (20 mM Tris–HCl [pH 7.5], 150 mM NaCl, 0.05% Tween 20), the membrane was incubated with either MPH antisera at a 1:1,000 dilution in TBST buffer. Subsequently, the membrane was incubated with alkaline phosphatase-conjugated goat anti-rabbit IgG antibody (Promega, Madison, WI, USA) at a 1:2,000 dilution. The membrane

was then stained with nitroblue tetrazolium and 5-bromo-4-chloro-3-indolylphosphate in alkaline phosphatase buffer (100 mM Tris–HCl, 100 mM NaCl; pH 9.0) for visualizing antigen–antibody conjugates.

Whole-cell activity assay

Induced cells were suspended in a 100-mM phosphate buffer (pH 7.4) and diluted to an OD₆₀₀ of 1.0. MPH activity assay mixtures (1 ml, 3% methanol) contained 50 μg ml⁻¹ methyl parathion (added from a 10-mg ml⁻¹ methanol stock solution), 960 μl of a 100-mM phosphate buffer (pH 7.4), and 10 μl of cells. Changes in absorbance (405 nm) were measured for 3 min at 30 °C using a Beckman DU800 spectrophotometer. Activities were expressed as units

(1 μmol of *p*-nitrophenol formed per minute) per OD600 whole cells ($\epsilon_{405}=17,700 \text{ M}^{-1} \text{ cm}^{-1}$ for *p*-nitrophenol).

Stability of resting cultures

Cells were grown in 50 ml of LB medium supplemented with 0.1 mM IPTG and 100 $\mu\text{g ml}^{-1}$ ampicillin for 2 days, washed twice with 50 ml of 150 mM NaCl solution, resuspended in 5 ml of 100 mM phosphate buffer (pH 7.4) and incubated in a shaker at 25 °C. Over a 2-week period, 0.1 ml of samples were removed each day. Samples were centrifuged and resuspended in 0.1 ml of 100 mM phosphate buffer (pH 7.4). MPH activity assays were conducted as described above.

Results

Construction of plasmids with different carrier peptides

PCR cloning was used to generate the recombinant enzymes containing carrier peptides. In this work, we analyzed the influence of various leader peptides on activity yields. The cleavage site prediction was performed using SignalP 3.0 Server (Emanuelsson et al. 2007). The SignalP analysis of all three leader peptides showed that the additional amino acids between the leader peptides are not expected to influence cleavage position. For successful surface presentation of MPH by the AIDA-1 autotransporter, pUADM18 encoding an artificial precursor was constructed. This precursor consists of a signal peptide at the N-terminus, the passenger (MPH protein), a linker region, and the β -barrel structure of the AIDA translocator (Fig. 1). To explore which anchor motif is more efficient to target MPH onto the surface of *E. coli*, the Lpp–OmpA and InaV protein were also employed as an anchoring motif for comparison. The maps and names of all of the constructs used in this study are illustrated in Fig. 1.

Production of whole-cell catalyst and Western blot analysis

To confirm the present of MPH on the expected compartment, the MPH were analyzed by Western blot. Samples

were separated on SDS-PAGE (12%) and probed by immunoblotting with MPH antisera. The mature-size MPH (32 kDa) was found in periplasmic fraction. However, no specific band was detected with the control cells carrying pUC18 (Fig. 2a). To examine whether MPH fusions was successfully synthesized on the cell surface, the production of MPH fusion protein were fractionated into whole-cell lysate and outer membrane fraction and the fractions analyzed by Western blot analyses using MPH antiserum. A specific band corresponding to MPH fusion protein (INPNC–MPH, 68 kDa; lpp–OmpA–MPH, 49 kDa; MPH–AIDA, 85 kDa) was detected in the outer membrane fraction (Fig. 2b). Target proteins were not detected in the outer membrane of the negative controls (Fig. 2b).

Effect of different carrier peptides on whole-cell activity

During the past few years, much progress has been made to improve the whole-cell biocatalyst, not only in the cytoplasm, but also in other cellular compartments (in the periplasm or outer membrane) (Kang et al. 2006; Shimazu et al. 2001b). In the present work, two different expression systems were investigated for the whole-cell activity of MPH. Firstly, three different leader peptides were compared: DsbA, PhoA, and TorA. The MPH activities obtained with the three distinct pathway, using JM109 as the host cell, are shown in Table 2. Our results indicate that the most efficient leader peptide–MPH gene combination was that based on TorA, with a threefold higher activity level compared with the cytosolic-expressing control vector. The strain expressing PhoA–MPH increased 2.3-fold whole-cell activities compared to the cytosolic-expressing control strain, reaching a level of 0.644 U/OD600; the strain expressing DsbA–MPH exhibited the lowest (2.1-fold) whole-cell activity among the three periplasmic expression systems. Thus, there are no major differences in the ability of phoA or DsbA signal peptide on the secretion of recombinant protein into the periplasmic space.

To explore which anchor system would improve activity of MPH on the cell surface, we compared the efficiency of targeting MPH using three different anchors. The anchor

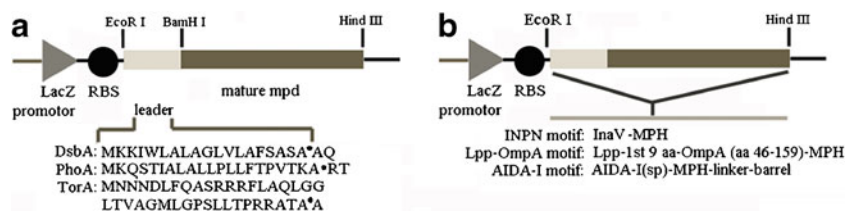
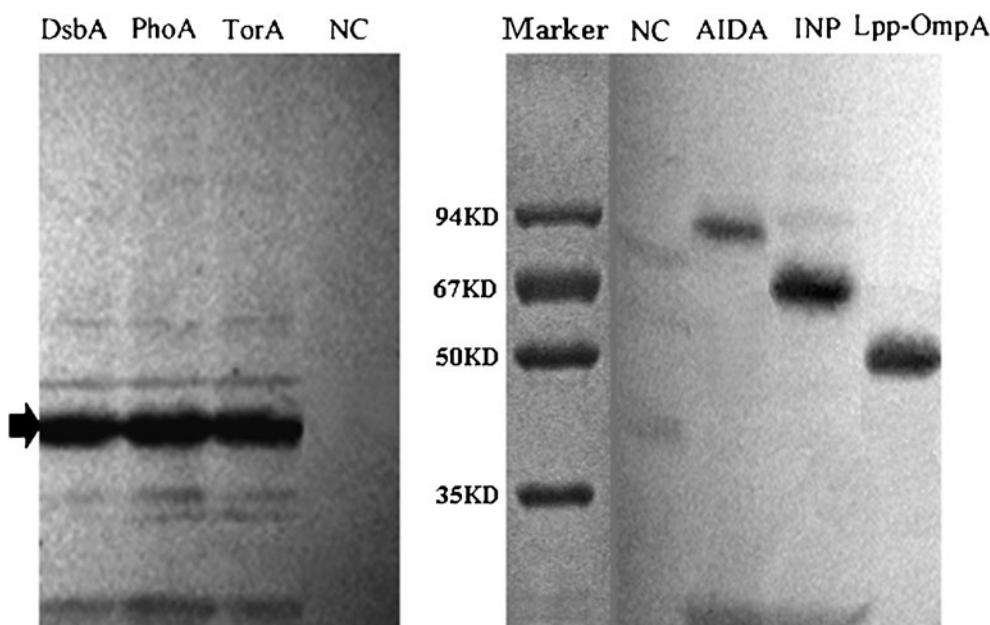


Fig. 1 Plasmids harboring the *mpd* gene. **a** The gene cassettes harboring the genes encoding various signal peptides, *mpd* gene encoding methyl parathion hydrolase, and the cleavage sites are shown. The gene cassettes were cloned into pUC18 plasmid. The cleavage site prediction was performed using SignalP 3.0 Server. The predicted

cleavage sites are stated. **b** The gene cassettes harboring the genes encoding various surface display motifs and *mpd* gene encoding methyl parathion hydrolase are shown. The gene cassettes were cloned into pUC18 plasmid. For construction processes, refer to “Material and methods”

Fig. 2 a Western blot analysis of soluble MPH in periplasmic fraction using different leader peptides. The position of mature-size MPH is indicated by an *arrow*. **b** Western blot analysis of expressed MPH on outer membrane fraction using different motifs. *NC* negative control (JM109/pUC18). MPH proteins were separated by reducing SDS-PAGE and detected using anti-MPH serum



system based on the autodisplay protein AIDA-I was developed for cell surface display of functional MPH in this work. The activity of cells expressing the MPH–AIDA-I fusions was compared to cells with surface-displayed MPH using two other fusion anchors. As shown in Table 2, the whole-cell activity based on AIDA-I was twofold lower than using the Lpp–OmpA anchor. The whole-cell activity based on InaV anchor was exhibited best, 2.4-fold higher activity compared to the AIDA-I anchor. Overall, the surface display expression system yielded one to three times whole-cell activity than the periplasmic expression system (Table 2).

Host cell comparison

Since *E. coli* strains differ in their ability to promote the expression of cloned genes, selection of a host strain is an

important factor that cannot be neglected. In this work, expression vector was used to transform the following strains: XL1-blue, BL21 (DE3), UT5600, and JM109. Whole-cell activity was carried out as mentioned above. The activity obtained in JM109 was higher than those obtained using the same vector in other strains and 7.2-fold higher compared with the control vector in XL-blue (Table 2). We would like to note that both *OmpT*-negative and *OmpT*-positive mutant strains of *E. coli* can be used to display recombinant proteins into cell surface. The surface display of the recombinant passenger protein can be verified and quantified in an *ompT*-negative host. However, the *OmpT*-positive host would result in the secretion of the passenger into the supernatant (Jose et al. 2001; Maurer and Meyer 1997). Therefore, *OmpT*-positive strains (XL1-blue and JM109) were not used to display fusion protein MPH–AIDA in this work.

Table 2 Analysis of whole-cell activity of various hosts, utilizing the expression vectors containing different carrier peptides

Whole-cell activity (U/OD ₆₀₀)	Periplasmic secretion			Surface display			Cytoplasmic expression
	DsbA	PhoA	TorA	INPN	Lpp–OmpA	AIDA ^b	
JM109	0.588 (210%)	0.644 (230%)	0.893 (319%)	1.96 (700%)	1.63 (582%)	–	0.280 (100%) ^a
XL-blue	0.582 (208%)	0.635 (227%)	0.891 (318%)	1.91 (682%)	1.59 (568%)	–	0.271
BL21(DE3)	0.571 (204%)	0.613 (219%)	0.888 (317%)	1.87 (668%)	1.52 (543%)	0.803 (287%)	–
UT5600	0.590 (211%)	0.640 (228%)	0.797 (285%)	1.95 (696%)	1.65 (589%)	0.812 (290%)	–

^a The whole-cell activity of host JM109 containing pUM18 was used as 100%. Activity on other host was compared with it

^b Both *OmpT*-negative (UT5600 and BL21(DE3)) and *OmpT*-positive (XL1-blue and JM109) strains of *E. coli* can be used to display recombinant proteins into cell surface. The surface display of the recombinant passenger protein can be verified and quantified in an *ompT*-negative host. However, the *OmpT*-positive host would result in the secretion of the passenger into the supernatant. Therefore, *OmpT*-positive strains (XL1-blue and JM109) were not used to display fusion protein MPH–AIDA in this work

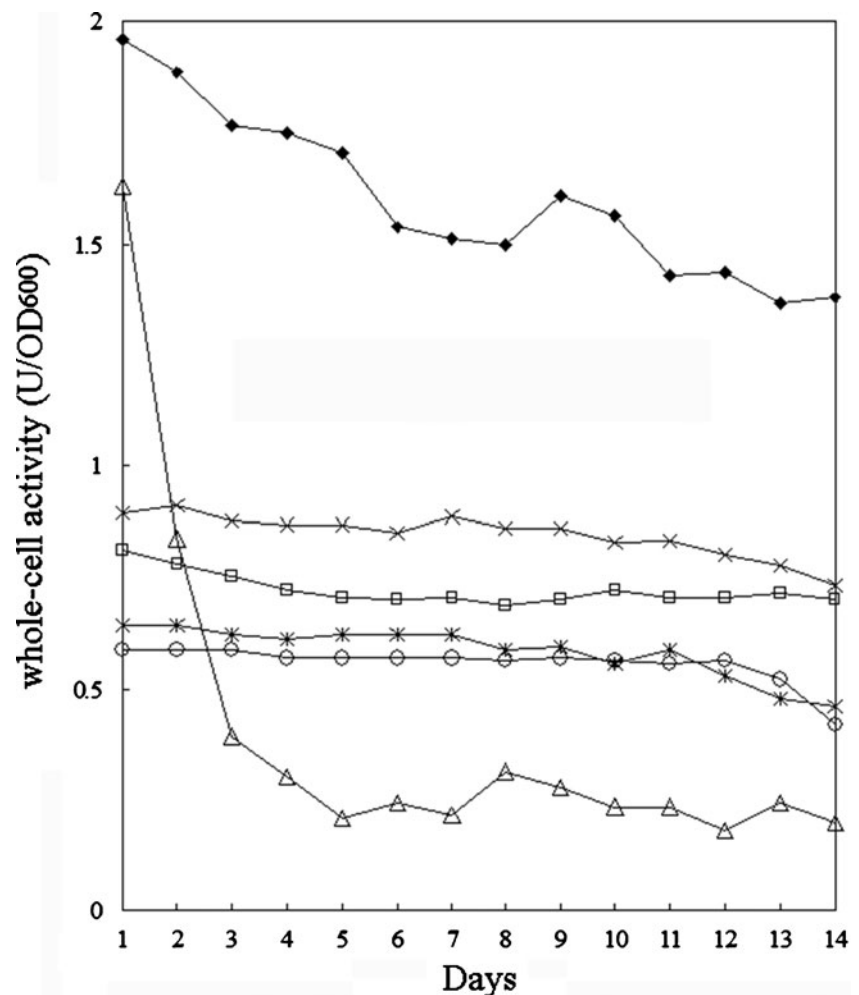
Stability of whole-cell activity

One of the major problems associated with whole-cell activity of MPH using signal system or anchor system is the instability observed in term of cell viability and MPH activity. To investigate MPH stability of strains, whole-cell activity was determined periodically over a 2-week period. As shown in Fig. 3, the cytoplasmic expression strain showed steadily decreasing MPH activity over the 2-week period, indicating proteolysis of MPH proteins in the cytoplasm. However, importantly, whole-cell MPH activity was stably maintained in the strain expressing periplasmic MPH or expressing MPH fusion on surface.

Discussion

Purified enzymes tend to be high in cost due to purification procedures, making the process uneconomical. Therefore, we often have the option of using the whole cell as the biocatalyst without going through the purification process.

Fig. 3 Remaining whole-cell MPH activities of the cells harboring periplasmic and surface MPH proteins under resting cell incubations. *Diamond*, cells carrying pINCM18; *triangle*, cells carrying pULOM18; *square*, cells carrying pUADM18; *multiplication sign*, cells carrying pUTM18; *asterisk*, cells carrying pUPM18; *circle*, cells carrying pUDM18



In fact, if the enzyme is not secreted, it requires that substrate be transported across the cell wall. To overcome the substrate transport barrier, various strategies to enhance whole-cell biocatalytic efficiency have been developed, including treatment of cells with permeabilizing agents, surface display by anchoring motif, and periplasmic secretion by leader peptide (Martina et al. 2011; Kang et al 2005; Kang et al; Richins et al 1997; Shimazu et al 2001a).

In this study, different leader peptides using the periplasmic pathways were compared in regard to MPH activity levels and production yields of soluble MPH. The impact on MPH display was evaluated by the production of MPH in periplasm using three different leader peptides and subsequent analysis by Western blot. First, the yields of soluble MPH were not affected by the choice of leader. This indicates that all leaders do not limit translocation of MPH. When the stability of whole-cell activity was analyzed, the use of all pathways offered the stability of functional MPH, with the Tat pathway seeming to be slightly better suited. However, whole-cell activity produced with Sec and SRP leader peptides did not lead to significant differences. This is

the first demonstration that the DsbA and PhoA pathway are applicable for MPH secretion and OPs detoxification. The results indicated that periplasmic expression reduced the substrate diffusion limitation experienced in whole-cell biocatalyst systems. In addition, with the protection of cell envelopes, whole-cell MPH activity in the periplasmic-secreting strain was generally more stable than in the surface-displaying strain (Fig. 3).

The first comparison of the impact of different anchors on surface display was done by Richard et al. (1997) who compared the special activity and stability of OPH. They compared the InaV-based anchor to the Lpp–OmpA anchor by Western blot showing the different display levels, according to the results shown in this work, but the AIDA-I anchor was not demonstrated. In contrast to the InaV and Lpp–ompA, AIDA-I occurs naturally in *E. coli* and therefore was considered a superior tool for surface display in this homologous host. In this lab, functional display of OPH-green fluorescent protein has been demonstrated using the AIDA-I transporter (Li et al. 2008). In this work, comparison was carried out among them in the similar experimental condition. According to the result, no major differences were observed between the different leader peptides regarding the secretion of MPH into the periplasm, except for more stability. The results showed that ice nucleation protein (InaV) was more efficient in targeting proteins to the cell surface in the three anchors. Compare to InaV, one drawback in using the Lpp–OmpA anchor is that it causes membrane instability leading to cell lysis. The increased expression level of the InaV-based anchor system may be the result of improved interaction with the outer membrane. The InaV anchor offers superior stability, showing no sign of cell lysis. Resting cultures maintained close to 80% activity after 2-week incubations. A successful display system must have a number of crucial features. It should have an efficient carrier peptide to allow premature fusion protein to go through the inner membrane and a strong anchoring structure to keep target proteins on the cell surface without detachment. In addition, it should be compatible with the foreign sequences and be resistant to attack by proteases. Taken together, our results suggest that ~two to sevenfold whole-cell activity could be promoted efficiently when comparing with intracellular expression. The surface display system seemed to be more efficient in promoting the whole-cell activity when compared to the periplasmic expression (Table 2).

Selection of a host strain for surface display is an important factor that cannot be neglected. A good host should be compatible with the protein to be displayed and should be easy to cultivate without cell lysis. Also, the host strain should have low activities of cell wall associated and extracellular proteases. For Gram-negative bacteria, including *E. coli*, the fragility of outer membrane caused by the display

of proteins can be a problem. Nevertheless, *E. coli* is still an attractive host because the availability various genetic tools and mutant strains and the high transformation efficiency.

In conclusion, six different carrier proteins were selected for the transport of proteins. The use of different carriers resulted in different whole-cell activities. The surface display expression system yielded one to three times more whole-cell activity than did the periplasmic expression system. However, the later showed the superior stability. Taking all the factors into consideration, the InaV anchor provides higher level of surface expression as well as superior stability. This carrier may be more applicable for the whole-cell degradation of organophosphates. In addition, it provides a useful reference for other whole-cell biocatalysts application.

Acknowledgments This work was financially supported by the 863 Hi-Tech Research and Development Program of the People's Republic of China (no. 2007AA06Z335; no. 2009AA06A417-02).

References

- Bae W, Wu CH, Kostal J, Mulchandani A, Chen W (2003) Enhanced mercury biosorption by bacterial cells with surface-displayed MerR. *Appl Environ Microbiol* 69:3176–3180
- Chu YF, Hsu CH, Soma PK, Lo YM (2009) Immobilization of bioluminescent *E. coli* cells using natural and artificial fibers treated with polyethyleneimine. *Bioresour Technol* 100:3167–74
- DeLisa MP, Tullman D, Georgiou G (2003) Folding quality control in the export of proteins by the bacterial twin-arginine translocation pathway. *Proc Natl Acad Sci* 100:6115–6120
- Emanuelsson O, Brunak S, Heijne G, Nielsen H, Emanuelsson O (2007) Locating proteins in the cell using TargetP, SignalP, and related tools. *Nat Protocols* 2:953–971
- Fu GP, Cui ZL, Huang TT, Li SP (2004) Expression, purification, and characterization of a novel methyl parathion hydrolase. *Protein Expr Purif* 36:170–176
- Jose J, Hannemann F, Bernhardt R (2001) Functional display of active bovine adrenodoxin on the surface of *E. coli* by chemical incorporation of the 2Fe-2S cluster. *ChemBiochem* 2:695–701
- Kang DG, Choi SS, Cha HJ (2006) Enhanced biodegradation of toxic organophosphate compounds using recombinant *Escherichia coli* with Sec pathway-driven periplasmic secretion of organophosphorus hydrolase. *Biotechnol Prog* 22:406–410
- Kang DG, Lim GB, Cha HJ (2005) Functional periplasmic secretion of organophosphorous hydrolase using the twin-arginine translocation pathway in *Escherichia coli*. *J Biotechnol* 118:379–385
- Katahira S, Mizuike A, Fukuda H, Kondo A (2006) Ethanol fermentation from lignocellulosic hydrolysate by a recombinant xylose- and celluloligosaccharide-assimilating yeast strain. *Appl Microbiol Biotechnol* 72:1136–1143
- Lee W, Wood TK, Chen W (2006) Engineering TCE-degrading rhizobacteria for heavy metal accumulation and enhanced TCE degradation. *Biotechnol Bioeng* 95:399–403
- Li C, Zhu Y, Benz I, Schmidt MA, Chen W, Mulchandani A, Qiao CL (2008) Presentation of functional organophosphorus hydrolase fusions on the surface of *Escherichia coli* by the AIDA-I auto-transporter pathway. *Biotechnol Bioeng* 99:485–490

- Li L, Kang DG, Cha HJ (2004) Functional display of foreign protein on surface of *Escherichia coli* using N-terminal domain of ice nucleation protein. *Biotechnol Bioeng* 85:214–221
- Martina LM, Ruiza CA, Andresa M, Catalana J (2011) Permeabilization of *trigonopsis variabilis* for enhanced D-amino acid oxidase activity. *Chemical Engin Commun* 198:516–529
- Maurer J, Meyer TF (1997) Autodisplay: one-component system for efficient surface display and release of soluble recombinant proteins from *Escherichia coli*. *J Bacteriol* 179:794–804
- Noureddini H, Gao X, Philkana RS (2005) Immobilized *Pseudomonas cepacia* lipase for biodiesel fuel production from soybean oil. *Bioresource Technology* 96:769–777
- Qin J, Song L, Brim H, Daly MJ, Summers AO (2006) Hg(II) sequestration and protection by the MerR metal-binding domain (MBD). *Microbiol* 152:709–719
- Rani NL, Lalithakumari D (1994) Degradation of methyl parathion by *Pseudomonas putida*. *Can J Microbiol* 40:1000–1006
- Richins RD, Kaneva I, Mulchandani A, Chen W (1997) Biodegradation of organophosphorus pesticides by surface-expressed organophosphorus hydrolase. *Nat Biotechnol* 15:984–987
- Sambrook J, Russell DW (2003) *Molecular cloning: a laboratory manual*, 3rd edn. Science, Beijing
- Shigechi H, Koh J, Fujita Y, Matsumoto T, Bito Y, Ueda M, Satoh E, Fukuda H, Kondo A (2004) Direct production of ethanol from raw corn starch via fermentation by use of a novel surface-engineered yeast strain codisplaying glucoamylase and α -amylase. *Appl Environ Microbiol* 70:5037–5040
- Shimazu M, Mulchandani A, Chen W (2001a) Cell surface display of organophosphorus hydrolase using ice nucleation protein. *Biotechnol Prog* 17:76–80
- Shimazu M, Mulchandani A, Chen W (2001b) Simultaneous degradation of organophosphorus pesticides and *p*-nitrophenol by a genetically engineered *Moraxella sp.* with surface-expressed organophosphorus hydrolase. *Biotechnol Bioeng* 76:318–324
- Thomas JD, Daniel RA, Errington J, Robinson C (2001) Export of active green fluorescent protein to the periplasm by the twin-arginine translocase (Tat) pathway in *Escherichia coli*. *Mol Microbiol* 39:47–53
- Yang C, Cai N, Dong M, Jiang H, Li J, Qiao C, Mulchandani A, Chen W (2008) Surface display of MPH on *Pseudomonas putida* JS 4444 using ice nucleation protein and its application in detoxification of organophosphate. *Biotechnol Bioeng* 99:30–37
- Yang C, Freudl R, Qiao C (2009) Export of methyl parathion hydrolase to the periplasm by the twin-arginine translocation pathway in *Escherichia coli*. *J Agric Food Chem* 57:8901–5
- Yang C, Freudl R, Qiao C, Mulchandani A (2010) Cotranslocation of methyl parathion hydrolase to the periplasm and of organophosphorus hydrolase to the cell surface of *Escherichia coli* by the Tat pathway and ice nucleation protein display system. *Appl Environ Microbiol* 76:434–40
- Yang C, Liu N, Guo XM, Qiao CL (2006) Cloning of *mpd* gene from a chlorpyrifos-degrading bacterium and use of this strain in bioremediation of contaminated soil. *FEMS Microbiol Lett* 265:118–125
- Zhang RF, Cui ZL, Zhang XZ, Jiang JD, Gu JD, Li SP (2006) Cloning of the organophosphorus pesticide hydrolase gene clusters of seven degradative bacteria isolated from a methyl parathion contaminated site and evidence of their horizontal gene transfer. *Biodegradation* 17:465–472